Interstitials in compositionally complex alloys

Ian Baker,* Blazej Grabowski, Sergiy V. Divinski, Xi Zhang, and Yuji Ikeda

The effects of interstitial alloying on the mechanical and diffusive properties of compositionally complex alloys (CCAs), including high-entropy alloys (HEAs), are reviewed. The solubility of interstitial elements in CCAs can be extraordinarily high, a feature corroborated by *ab initio* density functional theory simulations. The yield stresses, work-hardening rates, and Hall–Petch slopes of CCAs are normally reported to increase due to interstitial alloying. In some CCAs, interstitial alloying has been found to enhance both strength and ductility, thus circumventing the traditional tradeoff between these properties. Self-diffusivities of the HEA CoCrFeMnNi are found to show complex dependences on interstitial C concentration as well as on temperature. Some CCAs with Laves phase or body-centered cubic crystal structures show potential as hydrogen-storage materials, with both experimental and computational research in this area steadily increasing. Based on the insights obtained, possible directions for further studies on the impacts of interstitial alloying in CCAs are suggested.

Introduction

Independently, but almost simultaneously, Cantor et al.[1] and Yeh et al.[2] demonstrated that multielement alloys of equiatomic proportions could be cast as single-phase materials. Based on the idea that the resulting high configurational entropy would counterbalance the enthalpy of intermetallic phase formation, thus avoiding second phase formation, Yeh et al.[2] named these novel materials high-entropy alloys (HEAs), which they defined as containing at least five elements with concentrations from 5–35 at.%. Subsequently, the definition became more loosely used, and currently many papers have utilized the term HEA even when some elements were present at less than 5 at.% or when only four elements were present. Around the same time,[3] interest emerged in *multiphase* multielement alloys with elemental concentrations from 5–35 at.%. Such alloys have several different names, including multi-principal component alloys, multi-principal element alloys, and compositionally complex alloys (CCAs), a term that we will use here. We note that, while many as-cast HEAs are single-phase, upon subsequent annealing, one or more phases can precipitate.[4] Thus, we could consider HEAs as a class on CCAs, which are often metastable.

Interstitials can produce a wide range of effects depending on the alloy system. They can, for example (1) alter the phase equilibria,[5–7] including stabilizing metastable phases; (2) change the microstructure (e.g., decrease the grain size);[8] (3) modify stacking-fault energies;[9] (4) change mechanical properties;[10] and (5) affect the diffusion behavior of substitutional atoms.[11–13] Some of these effects have been barely studied for CCAs and are ripe for exploration. A recent paper[10] has intensively reviewed the effects of interstitial alloying on the mechanical properties of HEAs.

In this article, we review the effects of interstitial alloying in CCAs, including also their solubilities and diffusive properties. Over the last few years, these properties have been investigated not only by experiments but also by simulations, particularly those based on density functional theory (DFT), which can provide physical insights and explanations on the experimentally observed phenomena. Such recent DFT-based studies of interstitials in CCAs are also reviewed. Further, we provide an overview of a potential application of some CCAs for hydrogen storage, where a large amount of hydrogen can be accommodated in their interstitial sites.[14]

Ian Baker, Thayer School of Engineering, Dartmouth College, Hanover, USA; Ian.Baker@dartmouth.edu
Blazej Grabowski, Institute for Materials Science, University of Stuttgart, Stuttgart, Germany; blazej.grabowski@imw.uni-stuttgart.de
Sergiy V. Divinski, Institute of Materials Physics, University of Münster, Münster, Germany; divin@uni-muenster.de
Xi Zhang, Institute for Materials Science, University of Stuttgart, Stuttgart, Germany; xi.zhang@imw.uni-stuttgart.de
Yuji Ikeda, Institute for Materials Science, University of Stuttgart, Stuttgart, Germany; yuji.ikeda@imw.uni-stuttgart.de
*Corresponding author
doi:10.1557/s43577-023-00558-9

© The Author(s) 2023

Large solubility of interstitals in CCAs

The solubility of the interstitial elements such as boron, carbon, hydrogen, nitrogen, oxygen, and sulfur in elemental metals is generally quite low.[15] Nevertheless, even these very low concentrations of interstitials can affect ductility (e.g., carbon can lead to blue brittleness in steels[16] and sulfur can embrittle grain boundaries in nickel).[17] Although the solubilities of interstitial elements are low, the interstitial strengthening per atomic percent can be very high, particularly in body-centered cubic (bcc) metals.[18] In contrast, the solubility of interstitials in CCAs can be quite substantial. Liu et al.[19] reported that ultrahigh strength can be achieved through a massive solid solution of interstital oxygen, carbon, and nitrogen (up to 12 at.%) in a ternary bcc TiNbZr alloy. Since in some conventional alloys, such as twinning-induced plasticity (TWIP) steels or stainless steels, interstitals can generally provide strengthening, a comprehensive understanding of the solubility of interstitials in CCAs as well as the related physics becomes an indispensable step to develop potentially high-strength CCAs.

The solubility of a solute at different sites in a given matrix can be estimated from the energy differences between the structures with and without the solute atoms, which can be directly computed via DFT. For elemental metals, these energies can be straightforwardly obtained by enumerating all possible types of substitutional and interstitial sites, as shown by the delta peaks in **Figure 1**a for a solute Co atom in pure Hf. For *concentrated* multicomponent systems, however, these solution (or solute formation) energies become very sensitive to the local chemical environments.[20–24] The resulting distributions of the calculated formation energies, the so-called "density of states" (DOS) describing the number of states with a formation energy within a small energy interval, generally exhibit a significant broadening as depicted by the blue and the red DOSs in Figure 1b for the $Al_{15}Hf_{25}Sc_{10}Ti_{25}Zr_{25}$ HEA.[20] Note that, as the chemical complexity becomes significant in HEAs, many local positions (both substitutional and interstitial) appear energetically favorable for Co (negative formation energy), indicating a considerable enhancement of the Co interstitial and substitutional solubilities (Figure 1c–d). Remarkably, the preferred type of site for Co to occupy reverses from pure Hf to the HEA, which changes the corresponding diffusion mechanism as well, as discussed in the section on diffusion below. Indeed, such a dramatic reversion of the Co partitioning between substitutional and interstitial sites was found[20] to start to occur in the ternary HfTiZr by the addition of Ti to binary HfZr. As shown in Figure 1e, the formation energies of the (octahedral) interstitial Co in ternary HfTiZr decrease with an increasing number of Ti atoms in the local neighborhood. The significant broadening of the DOS from HfZr to HfTiZr (right panel of Figure 1e) can be explained by the large relaxations of the interstitial Co (relaxed positions indicated by red dots in Figure 1f).

In general, the significant chemical complexity and lattice distortions in CCAs could potentially provide an increased number of energetically favorable interstitial positions and thus enhance the solubility of interstitials. On the other hand, the addition of more elements could increase the solution energies as well. A comprehensive understanding requires future studies for more CCAs.

Enhanced mechanical properties

The effects of interstitial alloying on quasistatic mechanical properties have been studied largely at room temperature with some work at 77 K, while there are few studies at higher

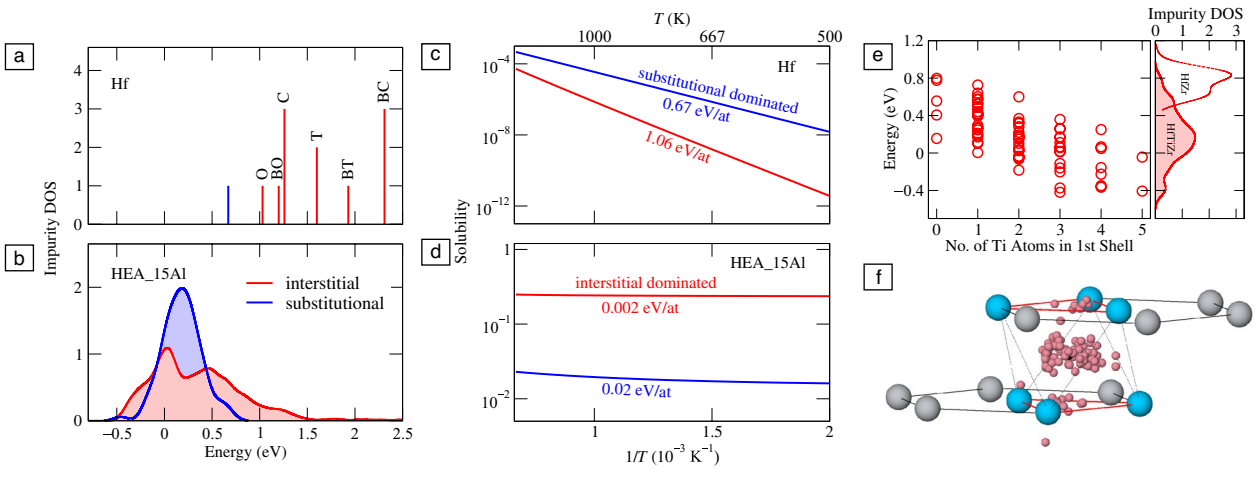

Figure 1. *Ab initio* predicted formation energies and solubilities of interstitial Co in pure hexagonal close-packed (HCP) Hf and HCP $Al_{15}Hf_{25}Sc_{10}Ti_{25}Zr_{25}$ high-entropy alloy (HEA_15Al). (a, b) Density of impurity states (impurity DOS), abbreviations: O, octahedral; BO, basal octahedral; C, crowdion; BC, basal crowdion; T, tetrahedral; BT, basal tetrahedral; (c, d) calculated temperature-dependent solubilities from the impurity DOS; (e) variation of the formation energies of the interstital Co with the number of Ti atoms in the 1st neighbor shell in ternary HfTiZr; (f) 3D illustration of the relaxations of the Co at different octahedral positions, where each red dot represents the relaxed position of an individual local chemical environment. (a–f) Adapted with permission from Reference 25.

temperatures. Work has largely been on single-phase alloys and there is a limited amount of data: obviously, results for multiphase alloys would be harder to interpret because the partitioning of the interstitial elements between different phases would have to be known. Even for single-phase HEAs, it is often hard to tease out the strengthening due to interstitial alloying because the interstitial could not only affect the strength directly but also indirectly by affecting the grain size.[8] A discussion of such issues when determining interstitial strengthening in polycrystals can be found in Reference 10.

Note that, regarding interstitials, it is not appropriate to assume that the as-prepared nominal composition is correct—the interstitial content should be accurately measured. The data we hereafter refer to are therefore derived not from nominal but from real compositions reported in the literature whenever possible.

Table I shows the increase in yield strength per at.%, $\Delta\sigma_y/\Delta c$, due to the addition of C or N for various HEAs in the face-centered cubic (fcc) phase at room temperature together with some data for traditional alloys. Note that the value may not always be accurate when it is derived from only one concentration of a dopant. Nevertheless, it is evident not only that interstitial strengthening can be quite substantial, but also that it is of a similar magnitude to the strengthening observed in traditional alloys. It has also been found that $\Delta\sigma_y/\Delta c$ for C or N can be 2.65–2.67 times larger at 77 K than at 293 K.[26,27] It is worth noting that the interstitial strengthening per atomic percent is comparable to that produced by substitutional atoms.[28]

The concentration dependence of interstitial strengthening is often described by either the Fleischer[39] or the Labusch[40] models, which were developed for *substitutional* atom strengthening. In these models, $\Delta\sigma_y$ is proportional to $c^{1/2}$ and $c^{2/3}$, respectively. However, tensile testing at room temperature of several CCAs containing several different concentrations of either C (i.e., $Fe_{40.4}Ni_{11.3}Mn_{34.8}Al_{7.5}Cr_6$,[9] NiCoCr,[32] $CoCr_{0.25}FeMnNi$),[27] or N (i.e., NiCoCr,[41] $Cr_{15}Fe_{46}Mn_{17}Ni_{22}$,[30] CoCrFeMnNi)[26] appears to show a $\sigma_y \propto c$ relationship. Tensile testings of several traditional alloys doped with N (i.e., Fe-17Cr-10Mn-5Ni,[42] Fe-18Cr-8Ni,[43] and Fe-27Cr-32Ni-3.3Mo) (tested at several temperatures within 78–873 K)[44] also seem to show this linear concentration dependence. The concentration dependence of the yield strength is an area worth studying further both experimentally and theoretically.

Chemical short-range ordering (SRO) should also be an important component of interstitial strengthening; interstitials could either increase or decrease the SRO. While recently direct observation of chemical SRO was reported for VCoNi,[45] it is still challenging to quantify SRO experimentally. To assess the impact of SRO on mechanical properties, it is essential to understand its effects on dislocation behavior.[46]

Table I. Increase in yield strength per atomic percent, $\Delta\sigma_y/\Delta c$, due to C or N for various fcc HEAs.

Alloy	Interstitial	T (K)	$\Delta\sigma_y/\Delta c$ (MPa/at.%)	Reference
$Fe_{40}Mn_{40}Co_{10}Cr_{10}$	C	RT	60	29
$Fe_{40.4}Ni_{11.3}Mn_{34.8}Al_{7.5}Cr_6$	C	RT	184	9
$Cr_{15}Fe_{46}Mn_{17}Ni_{22}$	N	RT	95	30
NiCoCr	N	293	81	31
NiCoCr	C	RT	140	32
CoCrFeMnNi	C	77	320	33
CoCrFeMnNi	C	293	120	33
CoCrFeMnNi	N	77	310	26
CoCrFeMnNi	N	293	117	26
$CoCr_{0.25}FeMnNi$	C	77	142	27
$CoCr_{0.25}FeMnNi$	C	293	64	27
TWIP steels	C	RT	26–42	34, 35
316 stainless steel	N	RT	~110	36
Fe-19Cr-10Ni	N	RT	~130	37
Fe-18Cr-10Ni	N	RT	~185	38

Work-hardening rate

While σ_y is related to how interstitial atoms affect dislocation motion, the change in work-hardening rate (WHR) is also affected by how interstitial atoms affect the cross-slip behavior, transformation to another phase, and the onset of twinning. The results of measurements of WHR in various studies on the same CCA are often contradictory. For example, Wu et al.[33] found that 0.5–2.0 at.% C increased the WHR of CoCrFeMnNi at both 77 K and 293 K by about 20 percent. In contrast, Li[47] found only a small increase in WHR with the addition of 0.25–0.90 at.% C, and Chen et al.[48] found 1.1 at.% C had little effect on WHR at 293 K. The impact could also depend on interstitial elements; for NiCoCr, Moravcik et al.[31] showed that 0.5 at.% N barely affects the WHR of the alloys with a grain size of 43–45 μm, while Shang et al.[32] showed that C did not affect the WHR up to 0.25 at.%, but increased at 0.75 at.% for alloys with the grain sizes of 140–160 μm.

When WHR increases were found in CCAs, these were related to observed changes in deformation behavior.[9,27,29,49] Again, modeling the effect of interstitials on the WHR of CCAs is an area that has seen little effort thus far.

Ductility

Interstitials can also affect the ductility. For example, for undoped CoCrFeMnNi with an average grain size of 0.65–155 μm,[50–52] the strain to failure ϵ_f is in the range of 0.4–0.7 at 293 K and tends to increase with increasing grain size. For $CoCrFeMnNiC_x$, Chen et al.[48] showed that the strain to failure ϵ_f increased from about 50% at $x = 0$ to about 60% at $x = 0.05$ (≈1 at.%), while for higher C concentrations up to $x = 0.2$ (≈4 at.%), ϵ_f starts to decrease drastically down to about 10 percent. In contrast, Wu et al.[33] showed a large decrease in ϵ_f due to the addition of only 0.5 at.% C for an alloy with an average grain size of ~115 μm both at 77 K and 293 K. The difference of the C impact between the two studies could be related to the average grain size. Similar

discrepancies of the results have been obtained also for $Fe_{40}Mn_{40}Co_{10}Cr_{10}$.[29,49] Neither C nor N had much effect on ϵ_f for large-grained NiCoCr.[31,32] Understanding the role of interstitials on the ductility is worthy of further efforts. The effect of interstitials is likely related to changes both in deformation mode and in WHR.

Hall–Petch slope

Interstitial elements in CCAs can dramatically change the Hall–Petch slope k by segregating to the grain boundaries. For example, the addition of 1 at.% C appears to increase k for equiatomic CoCrFeMnNi from 394–497 MPa· $\mu m^{-1/2}$ [50–52] to 935 MPa· $\mu m^{-1/2}$ [53] at room temperature. More dramatically, the addition of 0.47 at.% N to equiatomic NiCoCr increased k from 265 MPa· $\mu m^{-1/2}$ [54] to 748 MPa· $\mu m^{-1/2}$.[31] These observations indicate that the interstitial atoms made slip transmission across the grain boundaries more difficult although there were no measurements of the segregation behavior. It is worth noting that many studies, when calculating the strengthening from grain boundaries, ignore the fact that the Hall–Petch slope is changed by interstitials.

Slip mode

Interstitials can substantially change the slip behavior. For example, interstitial-free equiatomic CoCrFeMnNi deforms initially by dislocation glide, but at larger strains twinning also occurs.[51,52,55] There is some inconsistency of the impact of interstitial C alloying on the deformation mode as reported in different papers. Stepanov et al.[53] and Li[47] reported C reduced deformation twinning, while Wu et al.[33] reported the exact opposite. Chen et al.[48] reported that deformation twinning in $CoCrFeMnNiC_x$ increases from $x = 0$ to $x = 0.05$, but is not observed when the C content further increases to $x = 0.1$. A possible reason for the discrepancies is the extent of segregation of C to the grain boundaries; Stepanov et al.[53] and Li[47] reported that there was no C segregation at the grain boundaries, while Chen et al.[48] observed C segregation at the grain boundaries for $CoCrFeMnNiC_x$ when $x < 0.1$.

The impact of interstitial C depends also on the matrix composition. For nonequiatomic $CoCr_{0.25}FeMnNi$, Klimova et al.[27] reported that deformation twinning did not occur at all with or without C. For undoped $Al_{7.5}Cr_6Fe_{40.4}Mn_{34.8}Ni_{11.3}$, Wang et al.[9] observed initially wavy slip at low strains and cell formation at high strains. For the C-doped counterpart, in contrast, planar slip was observed at low strains, and a non-cell forming structure composed of the Taylor lattice, domain boundaries, and microbands was found at high strains. For $Fe_{40}Mn_{40}Co_{10}Cr_{10}$, Chen et al.[49] reported that C additions increased the deformation twinning.

The deformation modes of fcc austenitic alloys such as high-Mn steels often correlate with their stacking-fault energies.[56–60] *Ab initio* DFT simulations[22–24] suggest that, under the assumption of random distribution, interstitial alloying of C or N increases the stacking-fault energies of CoCrFeMnNi and $Al_{0.5}$CoFeMnNi, which supports potential changes of deformation modes for these alloys, for example, from deformation twinning to dislocation glide, due to the interstitial alloying.

Intriguing diffusion properties

In general, diffusion of interstitial elements such as C and N is studied using tracer diffusion (applying typically the ^{14}C radioisotope), chemical diffusion (using a diffusion couple technique), or mechanical spectroscopy methods.[61] Unfortunately, no such measurements have been reported so far for CCAs such as CoCrFeMnNi, although C diffusion in both bcc and fcc Fe-X (X = Cr, Mn, Co, Ni, etc.) binary alloys has been analyzed.[62,63]

Interestingly, interstitial C is found to impact *self*-diffusion of the substitutional elements in CoCrFeMnNi. Specifically, the tracer diffusion of the substitutional elements in $(CoCrFeNiMn)_{1-x}C_x$ was carefully measured by Lukianova et al.[11,13] Two different characteristic effects of the interstitial carbon on substitutional diffusion in these fcc alloys were distinguished. At the highest temperature of 1373 K, minor alloying by C ($x \leq 0.002$) retards substitutional diffusion. At lower temperatures and/or higher C concentrations ($x \geq 0.005$), an enhancement of the diffusion rates of all substitutional elements was observed. It was proposed that the lattice distortions caused by the interstitially dissolved carbon affect the self-diffusivities in the CoCrFeMnNi–C alloys.[13]

Interstitial alloying also affects vacancy diffusion in CCAs. Using positron annihilation measurements, Lu et al.[64] reported an enhancement of vacancy diffusion induced by C and N interstitial alloying in a CoCrFeMnNi HEA compared with the respective interstitial-free HEA.[65] The authors observed a reduction and narrowing of the migration barrier distribution for irradiation-induced vacancies.[64] This behavior was related to preferential localization of interstitial C and N to Mn- and Cr-rich regions in the alloy, which was predicted by DFT calculations.[64]

3*d* transition metallic elements such as Co, Fe, and Ni demonstrate unusual diffusion behavior in the α-phases of Ti, Zr, and Hf. They show not only high interstitial solubilities in the HCP lattices, but also extremely high diffusivities, which exceed those typical for self-diffusion by many orders of magnitude and are even faster than typical interstitials such as C, N, or B (only H diffusion rates in these α phases are higher).[66–68] Such *ultrafast* diffusion rates and the formation of vacancy–solute pairs affect self-diffusion, especially at lower temperatures[68] and are important for the mechanical properties. A recent study by Vaidya et al.[20] discovered the existence of ultrafast diffusion for Co in HCP AlScHfTiZr HEAs. Using DFT-informed calculations, this behavior was explained in terms of preferential interstitial solubility for Co in the HCP matrix and correspondingly a relatively small activation energy of diffusion.[20] Such behavior could be expected for other 3*d* transition elements (Fe or Ni) in HCP HEAs based on Hf, Ti, and Zr.

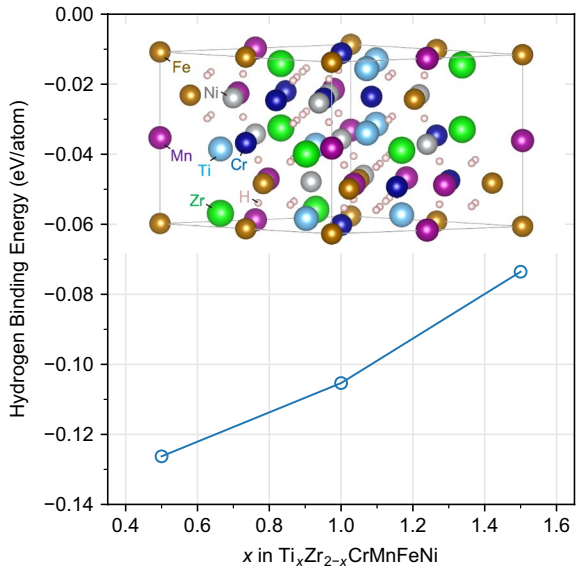

Figure 2. H binding energies in $Ti_xZr_{2-x}CrMnFeNi$ Laves-phase high-entropy alloys obtained by *ab initio* DFT simulations using supercell models.[74] A supercell model considered for the simulations is also shown.

Potential for hydrogen storage

An important potential application of CCAs is for hydrogen storage, where hydrogen atoms occupy the interstitial sites in the parent lattices. Here, we briefly introduce particularly noteworthy experimental results as well as the current status of *ab initio* DFT simulations of CCAs for hydrogen storage.

In 2010, Kao et al.[69] described the potential of the Ti_xV_y $MnFeCoZr_z$ HEA crystallizing in the hexagonal Laves phase (the C14 structure) for hydrogen storage. Subsequently, other Laves-phase CCAs were discovered to have potential for hydrogen storage.[70–74] In particular, Edalati et al.[71] synthesized C14-structured TiZrCrMnFeNi, which absorbed and desorbed hydrogen reversibly with a gravimetric storage capacity of 1.7 wt% at room temperature with rapid kinetics. Mohammadi et al.[74] extended the study to $Ti_xZr_{2-x}CrMnFeNi$ and found that the plateau pressure at room temperature in the pressure–composition–temperature (PCT) diagram increases with increasing Ti content. This also clearly demonstrates the possibility to tune the hydrogen-storage properties by modifying the composition of CCAs.

Other important CCAs for hydrogen storage are those with the bcc structure. In 2016, Sahlberg et al.[14] reported that bcc TiVZrNbHf could absorb hydrogen up to a hydrogen-to-metal (H/M) ratio of 2.5, comparable to H/M ratios in traditional hydrogen-storage alloys such as $LaNi_5$. Upon hydrogenation, TiNbVZrHf showed a phase transition from the bcc to the body-centered tetragonal (bct) phase. Later many other bcc CCAs with potential for hydrogen storage[75–79] were found to show similar phase transitions from the bcc to the bct or to the fcc phase upon hydrogenation. The high H/M ratios in these CCAs were ascribed to the hydrogen occupation of both the tetrahedral and the octahedral sites in the bct phase,[14] as later confirmed by neutron diffraction.[80,81] The increase of available sites is likely due to large lattice distortions in CCAs, indicating the high potential of CCAs for hydrogen storage by accommodating a large amount of hydrogen.

Compared with the rapid progress of experimental studies within only a few years, theoretical studies based on *ab initio* DFT simulations are still limited. Most of them are for bcc CCAs consisting mainly of refractory elements,[81–88] and only a few are for the Laves phases with sublattice-disordering.[74,89–91] For bcc HEAs, Hu et al.[85] showed a phase transition from bcc to fcc for TiZrNbMoHf upon hydrogenation in their DFT simulations, consistent with experiments.[81,84] For Laves-phase HEAs, Mohammadi et al.[74] demonstrated that the binding between hydrogen and metal atoms becomes weaker with increasing the Ti content for C14-structured $Ti_xZr_{2-x}CrMnFeNi$ (**Figure 2**). This is consistent with the experimentally observed increase of the plateau pressure in the PCT diagram with increasing Ti.[74]

Summary and outlook

We have briefly reviewed the effects of interstitial alloying on the mechanical and diffusive properties of CCAs as well as their potential application for hydrogen storage. Interstitial elements can show high solubilities in CCAs, which can affect their mechanical properties significantly. In particular, the yield strengths, WHRs, and Hall–Petch slopes of CCAs often increase due to interstitial alloying. Interstitial elements in CCAs sometimes also enhance the ductility. Self-diffusivities of CoCrFeMnNi are found to show complex dependences both on interstitial C concentration and on temperature. High solubilities of interstitial hydrogen offered by some CCAs provide the possibility for hydrogen storage with high capacities.

On the other hand, it has also been demonstrated that experimental results on the impact of interstitial alloying on mechanical properties are often contradictory with each other. To solve the discrepancies, further experimental studies with detailed characterization are suggested. Chemical SRO should also be important for interstitial strengthening, and it is thus essential to spend efforts to quantify and understand the role of SRO. Diffusion measurements of common interstitial solutes in fcc and bcc CCAs are so far missing and thus have to be performed. A theoretical assessment of the impact of the complex chemical environment on the diffusion rates of interstitial solutes has to be elaborated as well. From a simulation perspective, it is also promising to utilize machine learning interatomic potentials (MLIPs) fitted to DFT results to gain insight for mechanical and diffusive properties in CCAs from an atomistic viewpoint. For CCAs, MLIPs have shown great success for studying (e.g., finite-temperature thermodynamic properties,[92–94] lattice distortions,[95] and even magnetic properties)[96] almost to the accuracy of DFT calculations. It is thus promising to simulate interstitial alloying in CCAs also using MLIPs.

Acknowledgments

This project has received funding from the European Research Council (ERC) under the European Union's Horizon 2020 research and innovation programme (Grant Agreement No. 865855). Financial support from the Deutsche Forschungsgemeinschaft (DFG) via the research projects DI 1419/17-1 and GR 3716/5-1 is gratefully acknowledged. I.B. acknowledges support from the US National Science Foundation Grant No. 1758924. X.Z., B.G., and Y.I. acknowledge support by the state of Baden-Württemberg through bwHPC and the DFG through Grant No. INST 40/575-1 FUGG (JUSTUS 2 cluster). B.G. and Y.I. acknowledge support from the Stuttgart Center for Simulation Science (SimTech). Y.I. acknowledges support from the Faculty of Chemistry at the University of Stuttgart.

Conflict of interest

On behalf of all authors, the corresponding author states that there is no conflict of interest.

Open access

This article is licensed under a Creative Commons Attribution 4.0 International License, which permits use, sharing, adaptation, distribution and reproduction in any medium or format, as long as you give appropriate credit to the original author(s) and the source, provide a link to the Creative Commons license, and indicate if changes were made. The images or other third party material in this article are included in the article's Creative Commons license, unless indicated otherwise in a credit line to the material. If material is not included in the article's Creative Commons license and your intended use is not permitted by statutory regulation or exceeds the permitted use, you will need to obtain permission directly from the copyright holder. To view a copy of this license, visit http://creativecommons.org/licenses/by/4.0/.

References

1. B. Cantor, I. Chang, P. Knight, A. Vincent, *Mater. Sci. Eng. A* **375**, 213 (2004). https://doi.org/10.1016/j.msea.2003.10.257
2. J.W. Yeh, S.K. Chen, S.J. Lin, J.Y. Gan, T.S. Chin, T.T. Shun, C.H. Tsau, S.Y. Chang, *Adv. Eng. Mater.* **6**(5), 299 (2004). https://doi.org/10.1002/adem.200300567
3. J.A. Hanna, I. Baker, M.W. Wittmann, P.R. Munroe, *J. Mater. Res.* **20**(4), 791 (2005). https://doi.org/10.1557/JMR.2005.0136
4. F. Otto, A. Dlouhý, K. Pradeep, M. Kuběnová, D. Raabe, G. Eggeler, E. George, *Acta Mater.* **112**, 40 (2016). https://doi.org/10.1016/j.actamat.2016.04.005
5. Z. Wang, I. Baker, *Mater. Sci. Eng. A* **693**, 101 (2017). https://doi.org/10.1016/j.msea.2017.03.099
6. A. Semenyuk, E. Povolyaeva, V. Sanin, S. Zherebtsov, N. Stepanov, *Metals* (Basel) **12**(10), 1599 (2022). https://doi.org/10.3390/met12101599
7. G. Xiao, Q. Zhu, W. Yang, Y. Cui, S. Song, G.H. Cao, Z. Ren, *Sci. China Mater.* **66**, 257 (2023). https://doi.org/10.1007/s40843-022-2144-x
8. J.B. Seol, J.W. Bae, Z. Li, J.C. Han, J.G. Kim, D. Raabe, H.S. Kim, *Acta Mater.* **151**, 366 (2018). https://doi.org/10.1016/j.actamat.2018.04.004
9. Z. Wang, I. Baker, Z. Cai, S. Chen, J.D. Poplawsky, W. Guo, *Acta Mater.* **120**, 228 (2016). https://doi.org/10.1016/j.actamat.2016.08.072
10. I. Baker, *Metals* (Basel) **10**(5), 695 (2020). https://doi.org/10.3390/met10050695
11. O. Lukianova, Z. Rao, V. Kulitckii, Z. Li, G. Wilde, S. Divinski, *Scr. Mater.* **188**, 264 (2020). https://doi.org/10.1016/j.scriptamat.2020.07.044
12. E. Lu, J. Zhao, I. Makkonen, K. Mizohata, Z. Li, M. Hua, F. Djurabekova, F. Tuomisto, *Acta Mater.* **215**, 117093 (2021). https://doi.org/10.1016/j.actamat.2021.117093
13. O. Lukianova, V. Kulitckii, Z. Rao, Z. Li, G. Wilde, S. Divinski, *Acta Mater.* **237**, 118136 (2022). https://doi.org/10.1016/j.actamat.2022.118136
14. M. Sahlberg, D. Karlsson, C. Zlotea, U. Jansson, *Sci. Rep.* **6**(1), 36770 (2016). https://doi.org/10.1038/srep36770
15. T. Massalski, H. Okamoto, P. Subramanian, L. Kacprzak (eds.), *Binary Alloy Phase Diagrams*, 2nd edn. (ASM International, 1990). https://www.asminternational.org/online-catalog/alloy-phase-diagrams/-/journal_content/56/10192/57718G/PUBLICATION
16. M. Koyama, Y. Shimomura, A. Chiba, E. Akiyama, K. Tsuzaki, *Scr. Mater.* **141**, 20 (2017). https://doi.org/10.1016/j.scriptamat.2017.07.017
17. M. Všianská, M. Šob, *Prog. Mater. Sci.* **56**(6), 817 (2011). https://doi.org/10.1016/j.pmatsci.2011.01.008
18. P. Evans, *J. Less-Common Met.* **4**(1), 78 (1962). https://doi.org/10.1016/0022-5088(62)90062-0
19. C. Liu, W. Lu, W. Xia, C. Du, Z. Rao, J.P. Best, S. Brinckmann, J. Lu, B. Gault, G. Dehm, G. Wu, Z. Li, D. Raabe, *Nat. Commun.* **13**, 1102 (2022). https://doi.org/10.1038/s41467-022-28706-w
20. M. Vaidya, S. Sen, X. Zhang, L. Frommeyer, Ł. Rogal, S. Sankaran, B. Grabowski, G. Wilde, S.V. Divinski, *Acta Mater.* **196**, 220 (2020). https://doi.org/10.1016/j.actamat.2020.06.025
21. A.J. Samin, *J. Appl. Phys.* **128**(21), 215101 (2020). https://doi.org/10.1063/5.0028977
22. Y. Ikeda, I. Tanaka, J. Neugebauer, F. Körmann, *Phys. Rev. Mater.* **3**, 113603 (2019). https://doi.org/10.1103/PhysRevMaterials.3.113603
23. F. Kies, Y. Ikeda, S. Ewald, J.H. Schleifenbaum, B. Hallstedt, F. Körmann, C. Haase, *Scr. Mater.* **178**, 366 (2020). https://doi.org/10.1016/j.scriptamat.2019.12.004
24. Y. Ikeda, F. Körmann, *J. Phase Equilib. Diffus.* **42**, 551 (2021). https://doi.org/10.1007/s11669-021-00877-x
25. M. Vaidya, S. Sen, X. Zhang, L. Frommeyer, L. Rogal, S. Sankaran, B. Grabowski, G. Wilde, S. Divinski, *Acta Mater.* **196**, 220 (2020). https://doi.org/10.1016/j.actamat.2020.06.025
26. M. Klimova, D. Shaysultanov, A. Semenyuk, S. Zherebtsov, G. Salishchev, N. Stepanov, *J. Alloys Compd.* **849**, 156633 (2020). https://doi.org/10.1016/j.jallcom.2020.156633
27. M. Klimova, A. Semenyuk, D. Shaysultanov, G. Salishchev, S. Zherebtsov, N. Stepanov, *J. Alloys Compd.* **811**, 152000 (2019). https://doi.org/10.1016/j.jallcom.2019.152000
28. R.W.K. Honeycombe, *The Plastic Deformation of Metals*, 2nd edn. (Edward Arnold, London, 1984)
29. R. Wei, H. Sun, Z. Han, C. Chen, T. Wang, S. Guan, F. Li, *Mater. Lett.* **219**, 85 (2018). https://doi.org/10.1016/j.matlet.2018.02.065
30. M. Traversier, P. Mestre-Rinn, N. Peillon, E. Rigal, X. Boulnat, F. Tancret, J. Dhers, A. Fraczkiewicz, *Mater. Sci. Eng. A* **804**, 140725 (2021). https://doi.org/10.1016/j.msea.2020.140725
31. I. Moravcik, H. Hadraba, L. Li, I. Dlouhy, D. Raabe, Z. Li, *Scr. Mater.* **178**, 391 (2020). https://doi.org/10.1016/j.scriptamat.2019.12.007
32. Y. Shang, Y. Wu, J. He, X. Zhu, S. Liu, H. Huang, K. An, Y. Chen, S. Jiang, H. Wang, X. Liu, Z. Lu, *Intermetallics* **106**, 77 (2019). https://doi.org/10.1016/j.intermet.2018.12.009
33. Z. Wu, C. Parish, H. Bei, *J. Alloys Compd.* **647**, 815 (2015). https://doi.org/10.1016/j.jallcom.2015.05.224
34. O. Bouaziz, H. Zurob, B. Chehab, J.D. Embury, S. Allain, M. Huang, *Mater. Sci. Technol.* **27**(3), 707 (2011). https://doi.org/10.1179/026708309x12535382371852
35. E.E. Yang, "The Effect of Carbon Content on the Mechanical Properties and Microstructural Evolution of Fe-22Mn-C TWIP/TRIP Steels," Master's thesis, McMaster University (2010). http://hdl.handle.net/11375/9485
36. T. Masumura, Y. Seto, T. Tsuchiyama, K. Kimura, *Mater. Trans.* **61**(4), 678 (2020). https://doi.org/10.2320/matertrans.h-m2020804
37. R.P. Reed, *JOM* **41**(3), 16 (1989). https://doi.org/10.1007/bf03220991
38. K.J. Irvine, D.T. Llewellyn, F.B. Pickering, *J. Iron Steel Inst.* **199**, 153 (1961)
39. R. Fleischer, *Acta Metall.* **9**(11), 996 (1961). https://doi.org/10.1016/0001-6160(61)90242-5
40. R. Labusch, *Phys. Status Solidi B* **41**(2), 659 (1970). https://doi.org/10.1002/pssb.19700410221
41. I. Moravcik, N.S. Peighambardoust, A. Motallebzadeh, L. Moravcikova-Gouvea, C. Liu, J.M. Prabhakar, I. Dlouhy, Z. Li, *Mater. Charact.* **172**, 110869 (2021). https://doi.org/10.1016/j.matchar.2020.110869
42. J. Simmons, *Mater. Sci. Eng. A* **207**(2), 159 (1996). https://doi.org/10.1016/0921-5093(95)09991-3
43. R. Sandstrom, H. Bergqvist, *Scand. J. Metall.* **6**(4), 156 (1977)
44. M. Byrnes, M. Grujicic, W. Owen, *Acta Metall.* **35**(7), 1853 (1987). https://doi.org/10.1016/0001-6160(87)90131-3
45. X. Chen, Q. Wang, Z. Cheng, M. Zhu, H. Zhou, P. Jiang, L. Zhou, Q. Xue, F. Yuan, J. Zhu, X. Wu, E. Ma, *Nature* **592**(7856), 712 (2021). https://doi.org/10.1038/s41586-021-03428-z
46. S. Yin, Y. Zuo, A. Abu-Odeh, H. Zheng, X.G. Li, J. Ding, S.P. Ong, M. Asta, R.O. Ritchie, *Nat. Commun.* **12**(1), 4873 (2021). https://doi.org/10.1038/s41467-021-25134-0

47. Z. Li, *Acta Mater.* **164**, 400 (2019). https://doi.org/10.1016/j.actamat.2018.10.050
48. J. Chen, Z. Yao, X. Wang, Y. Lu, X. Wang, Y. Liu, X. Fan, *Mater. Chem. Phys.* **210**, 136 (2018). https://doi.org/10.1016/j.matchemphys.2017.08.011
49. L. Chen, R. Wei, K. Tang, J. Zhang, F. Jiang, L. He, J. Sun, *Mater. Sci. Eng. A* **716**, 150 (2018). https://doi.org/10.1016/j.msea.2018.01.045
50. G. Liu, D.H. Lu, X.W. Liu, F.C. Liu, Q. Yang, H. Du, Q. Hu, Z.T. Fan, *Mater. Sci. Technol.* **35**(4), 500 (2019). https://doi.org/10.1080/02670836.2019.1570679
51. F. Otto, A. Dlouhý, C. Somsen, H. Bei, G. Eggeler, E. George, *Acta Mater.* **61**(15), 5743 (2013). https://doi.org/10.1016/j.actamat.2013.06.018
52. S. Sun, Y. Tian, H. Lin, X. Dong, Y. Wang, Z. Wang, Z. Zhang, *J. Alloys Compd.* **806**, 992 (2019). https://doi.org/10.1016/j.jallcom.2019.07.357
53. N. Stepanov, D. Shaysultanov, R. Chernichenko, N.Y. Yurchenko, S. Zherebtsov, M. Tikhonovsky, G. Salishchev, *J. Alloys Compd.* **693**, 394 (2017). https://doi.org/10.1016/j.jallcom.2016.09.208
54. S. Yoshida, T. Bhattacharjee, Y. Bai, N. Tsuji, *Scr. Mater.* **134**, 33 (2017). https://doi.org/10.1016/j.scriptamat.2017.02.042
55. G. Laplanche, A. Kostka, O. Horst, G. Eggeler, E. George, *Acta Mater.* **118**, 152 (2016). https://doi.org/10.1016/j.actamat.2016.07.038
56. O. Grässel, L. Krüger, G. Frommeyer, L. Meyer, *Int. J. Plast.* **16**(10), 1391 (2000). https://doi.org/10.1016/S0749-6419(00)00015-2
57. G. Frommeyer, U. Brüx, P. Neumann, *ISIJ Int.* **43**(3), 438 (2003). https://doi.org/10.2355/isijinternational.43.438
58. D. Pierce, J. Jiménez, J. Bentley, D. Raabe, C. Oskay, J. Wittig, *Acta Mater.* **68**, 238 (2014). https://doi.org/10.1016/j.actamat.2014.01.001
59. O. Bouaziz, S. Allain, C. Scott, P. Cugy, D. Barbier, *Curr. Opin. Solid State Mater. Sci.* **15**(4), 141 (2011). https://doi.org/10.1016/j.cossms.2011.04.002
60. B.C.D. Cooman, Y. Estrin, S.K. Kim, *Acta Mater.* **142**, 283 (2018). https://doi.org/10.1016/j.actamat.2017.06.046
61. H. Mehrer, *Diffusion in Solids: Fundamentals, Methods, Materials, Diffusion-Controlled Processes*, Springer Series in Solid State Science, vol. 155 (Springer, Berlin, 2007). https://doi.org/10.1007/978-3-540-71488-0
62. A.A. Vasilyev, "Carbon Diffusion Coefficient in Complexly Alloyed Austenite," presented at the Materials Science & Technology Conference (MS&T'07), Detroit, MI, September 16–20, 2007. https://doi.org/10.13140/2.1.5050.9125.
63. A. Vasilyev, P.A. Golikov, *Mater. Phys. Mech.* **39**(1), 111 (2018). https://doi.org/10.18720/MPM.3912018_17
64. E. Lu, I. Makkonen, K. Mizohata, Z. Li, J. Räisänen, F. Tuomisto, *J. Appl. Phys.* **127**(2), 025103 (2020). https://doi.org/10.1063/1.5130748
65. M. Elsayed, R. Krause-Rehberg, C. Eisenschmidt, N. Eißmann, B. Kieback, *Phys. Status Solidi A* **215**(11), 1800036 (2018). https://doi.org/10.1002/pssa.201800036
66. H. Nakajima, M. Koiwa, *ISIJ Int.* **31**(8), 757 (1991). https://doi.org/10.2355/isijinternational.31.757
67. R. Perez, H. Nakajima, F. Dyment, *Mater. Trans.* **44**(1), 2 (2003). https://doi.org/10.2320/matertrans.44.2
68. C. Herzig, S. Divinski, Y. Mishin, *Metall. Mater. Trans. A* **33**(3), 765 (2002). https://doi.org/10.1007/s11661-002-0143-0
69. Y.F. Kao, S.K. Chen, J.H. Sheu, J.T. Lin, W.E. Lin, J.W. Yeh, S.J. Lin, T.H. Liou, C.W. Wang, *Int. J. Hydrogen Energy* **35**(17), 9046 (2010). https://doi.org/10.1016/j.ijhydene.2010.06.012
70. I. Kunce, M. Polanski, J. Bystrzycki, *Int. J. Hydrogen Energy* **38**(27), 12180 (2013). https://doi.org/10.1016/j.ijhydene.2013.05.071
71. P. Edalati, R. Floriano, A. Mohammadi, Y. Li, G. Zepon, H.W. Li, K. Edalati, *Scr. Mater.* **178**, 387 (2020). https://doi.org/10.1016/j.scriptamat.2019.12.009
72. R. Floriano, G. Zepon, K. Edalati, G.L. Fontana, A. Mohammadi, Z. Ma, H.W. Li, R.J. Contieri, *Int. J. Hydrogen Energy* **45**(58), 33759 (2020). https://doi.org/10.1016/j.ijhydene.2020.09.047
73. R. Floriano, G. Zepon, K. Edalati, G.L. Fontana, A. Mohammadi, Z. Ma, H.W. Li, R.J. Contieri, *Int. J. Hydrogen Energy* **46**(46), 23757 (2021). https://doi.org/10.1016/j.ijhydene.2021.04.181
74. A. Mohammadi, Y. Ikeda, P. Edalati, M. Mito, B. Grabowski, H.W. Li, K. Edalati, *Acta Mater.* **236**, 118117 (2022). https://doi.org/10.1016/j.actamat.2022.118117
75. J. Montero, C. Zlotea, G. Ek, J.C. Crivello, L. Laversenne, M. Sahlberg, *Molecules* **24**(15), 2799 (2019). https://doi.org/10.3390/molecules24152799
76. M.M. Nygård, G. Ek, D. Karlsson, M.H. Sørby, M. Sahlberg, B.C. Hauback, *Acta Mater.* **175**, 121 (2019). https://doi.org/10.1016/j.actamat.2019.06.002
77. M.M. Nygård, G. Ek, D. Karlsson, M. Sahlberg, M.H. Sørby, B.C. Hauback, *Int. J. Hydrogen Energy* **44**(55), 29140 (2019). https://doi.org/10.1016/j.ijhydene.2019.03.223
78. C. Zlotea, M. Sow, G. Ek, J.P. Couzinié, L. Perrière, I. Guillot, J. Bourgon, K. Møller, T. Jensen, E. Akiba, M. Sahlberg, *J. Alloys Compd.* **775**, 667 (2019). https://doi.org/10.1016/j.jallcom.2018.10.108
79. J. Montero, G. Ek, L. Laversenne, V. Nassif, G. Zepon, M. Sahlberg, C. Zlotea, *J. Alloys Compd.* **835**, 155376 (2020). https://doi.org/10.1016/j.jallcom.2020.155376
80. D. Karlsson, G. Ek, J. Cedervall, C. Zlotea, K.T. Møller, T.C. Hansen, J. Bednarčík, M. Paskevicius, M.H. Sørby, T.R. Jensen, U. Jansson, M. Sahlberg, *Inorg. Chem.* **57**(4), 2103 (2018). https://doi.org/10.1021/acs.inorgchem.7b03004
81. H. Shen, J. Zhang, J. Hu, J. Zhang, Y. Mao, H. Xiao, X. Zhou, X. Zu, *Nanomaterials* (Basel) **9**(2), 248 (2019). https://doi.org/10.3390/nano9020248
82. P. Li, J. Zhang, J. Hu, G. Huang, L. Xie, H. Xiao, X. Zhou, Y. Xia, J. Zhang, H. Shen, X. Zu, *J. Solid State Chem.* **297**, 121999 (2021). https://doi.org/10.1016/j.jssc.2021.121999
83. J. Hu, H. Shen, M. Jiang, H. Gong, H. Xiao, Z. Liu, G. Sun, X. Zu, *Nanomaterials* (Basel) **9**(3), 461 (2019). https://doi.org/10.3390/nano9030461
84. H. Shen, J. Hu, P. Li, G. Huang, J. Zhang, J. Zhang, Y. Mao, H. Xiao, X. Zhou, X. Zu, X. Long, S. Peng, *J. Mater. Sci. Technol.* **55**, 116 (2020). https://doi.org/10.1016/j.jmst.2019.08.060
85. J. Hu, J. Zhang, H. Xiao, L. Xie, H. Shen, P. Li, J. Zhang, H. Gong, X. Zu, *Inorg. Chem.* **59**(14), 9774 (2020). https://doi.org/10.1021/acs.inorgchem.0c00989
86. J. Zhang, J. Hu, H. Xiao, H. Shen, L. Xie, G. Sun, X. Zu, *Metals* (Basel) **11**(4), 553 (2021). https://doi.org/10.3390/met11040553
87. J. Hu, J. Zhang, H. Xiao, L. Xie, G. Sun, H. Shen, P. Li, J. Zhang, X. Zu, *Int. J. Hydrogen Energy* **46**(40), 21050 (2021). https://doi.org/10.1016/j.ijhydene.2021.03.200
88. J. Hu, J. Zhang, M. Li, S. Zhang, H. Xiao, L. Xie, G. Sun, H. Shen, X. Zhou, X. Li, P. Li, J. Zhang, L. Vitos, X. Zu, *J. Mater. Chem. A* **10**(13), 7228 (2022). https://doi.org/10.1039/d1ta10649j
89. S.B. Gesari, M.E. Pronsato, A. Visintin, A. Juan, *J. Phys. Chem. C* **114**(39), 16832 (2010). https://doi.org/10.1021/jp106036v
90. A. Robina Merlino, C. Luna, A. Juan, M. Pronsato, *Int. J. Hydrogen Energy* **41**(4), 2700 (2016). https://doi.org/10.1016/j.ijhydene.2015.10.077
91. A. Robina, P. Bechthold, A. Juan, C. Pistonesi, M. Pronsato, *Int. J. Hydrogen Energy* **43**(33), 16085 (2018). https://doi.org/10.1016/j.ijhydene.2018.06.131
92. B. Grabowski, Y. Ikeda, P. Srinivasan, F. Körmann, C. Freysoldt, A.I. Duff, A. Shapeev, J. Neugebauer, *NPJ Comput. Mater.* **5**(1), 80 (2019). https://doi.org/10.1038/s41524-019-0218-8
93. K. Gubaev, V. Zaverkin, P. Srinivasan, A.I. Duff, J. Kästner, B. Grabowski. Exploring the limits of machine-learned potentials for chemically complex multicomponent systems (2022), Preprint, https://doi.org/10.21203/rs.3.rs-2073581/v1
94. Y. Zhou, P. Srinivasan, F. Körmann, B. Grabowski, R. Smith, P. Goddard, A.I. Duff, *Phys. Rev. B* **105**(21), 214302 (2022). https://doi.org/10.1103/PhysRevB.105.214302
95. K. Gubaev, Y. Ikeda, F. Tasnádi, J. Neugebauer, A.V. Shapeev, B. Grabowski, F. Körmann, *Phys. Rev. Mater.* **5**(7), 073801 (2021). https://doi.org/10.1103/PhysRevMaterials.5.073801
96. I. Novikov, B. Grabowski, F. Körmann, A. Shapeev, *NPJ Comput. Mater.* **8**(1), 13 (2022). https://doi.org/10.1038/s41524-022-00696-9

Publisher's note Springer Nature remains neutral with regard to jurisdictional claims in published maps and institutional affiliations.

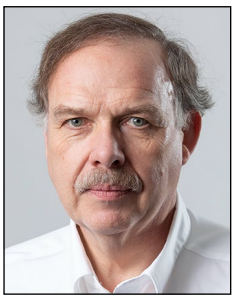

Ian Baker is the Sherman Fairchild Professor of Engineering and senior associate dean for research and graduate programs in the Thayer School of Engineering at Dartmouth College. He obtained his BA and DPhil degrees from the University of Oxford, UK. His research interests include the mechanical properties of high-entropy alloys and intermetallic compounds; recrystallization phenomena; Na-ion batteries, thermoelectric materials; the structure, chemistry, and properties of snow and ice; production and properties of nanocrystalline, particularly magnetic materials; nanoparticles and structural materials for biomedical applications. Baker can be reached by email at Ian.Baker@dartmouth.edu.

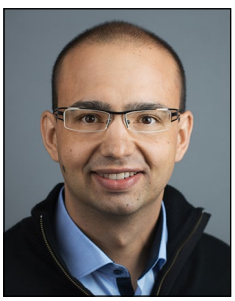

Blazej Grabowski is a professor at the Institute for Materials Science at the University of Stuttgart, Germany. He obtained his physics diploma in 2005 and completed his PhD degree at the Max-Planck-Institut für Eisenforschung (MPIE), Germany, in 2009. After a postdoctoral stay at the Lawrence Livermore National Laboratory, he became group leader at the MPIE in 2012, before moving to his professor position in 2019. His research focuses on machine learning potentials and *ab initio* simulations. His awards include a European Research Council (ERC) Starting Grant and a ERC Consolidator Grant. Grabowski can be reached by email at blazej.grabowski@imw.uni-stuttgart.de.

Sergiy V. Divinski leads the radiotracer laboratory at the Institute of Materials Physics at the University of Münster, Germany, which he joined as an Alexander von Humboldt Fellow in 1998. He graduated from Moscow Institute of Physics and Technology and received his PhD degree at the Institute of Metals Physics, Ukraine. His research is focused on kinetic and thermodynamic properties of interfaces in solids, diffusion phenomena in intermetallic compounds, effects of ordering on diffusion kinetic and diffusion mechanisms, interfaces in severely deformed materials. Divinski can be reached by email at divin@uni-muenster.de.

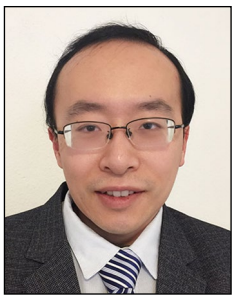

Xi Zhang is a postdoctoral researcher at the Institute for Materials Science at the University of Stuttgart, Germany. He received his PhD degree in materials science and engineering at Delft University of Technology, The Netherlands. After receiving his PhD degree, he worked as a postdoctoral researcher at Max-Planck-Institut für Eisenforschung, Germany. His research focuses mainly on *ab initio* density-functional-theory-based atomistic simulations of alloy thermodynamics and diffusion kinetics using the finite-temperature thermodynamic integration approach, machine learning interatomic potentials, and the kinetic Monte Carlo method. Zhang can be reached by email at xi.zhang@imw.uni-stuttgart.de.

Yuji Ikeda is a scientist at the University of Stuttgart, Germany. Before joining the university, he worked at the Max-Planck-Institut für Eisenforschung GmbH, Germany, and Kyoto University, Japan. He obtained his PhD degree from Kyoto University in 2013. His research focuses on mechanical properties, thermodynamical and dynamical stabilities, and hydrogen-storage properties of metals and alloys, including compositionally complex alloys, based on both first-principles simulations and machine learning interatomic potentials. Ikeda can be reached by email at yuji.ikeda@imw.uni-stuttgart.de.